Chaparro, M. A. E., Böhnel, H. N., Byrne, R., Nowaczyk, N., Molina-Garza, R. S., Park, J., Negendank, J. F. (2008): Palaeomagnetic secular variation and rock-magnetic studies of Holocene sediments from a maar lake (Hoya de San Nicolas) in Central Mexico. - Geophysical Journal International, 175, 2, pp. 462—476.

DOI: http://doi.org/10.1111/j.1365-246X.2008.03893.x

Geophys. J. Int. (2008) **175,** 462–476 doi: 10.1111/j.1365-246X.2008.03893.x

Palaeomagnetic secular variation and rock-magnetic studies of Holocene sediments from a maar lake (Hoya de San Nicolas) in Central Mexico

Marcos A. E. Chaparro,[1,2],* Harald N. Böhnel,[1] Roger Byrne,[3] Norbert R. Nowaczyk,[4] Roberto S. Molina-Garza,[1] Jungjae Park[3] and Jörg F. W. Negendank[4]

[1] *Centro de Geociencias-UNAM, Boulevard Juriquilla No. 3001, 76230 Querétaro, México, Mexico. E-mail: chapator@exa.unicen.edu.ar*
[2] *Instituto de Física Arroyo Seco (UNCPBA)-CONICET, Pinto 399, B7000GHG Tandil, Argentina*
[3] *Geography Department, 507 McCon Hall, University of California at Berkeley, Berkeley, CA 94720, USA*
[4] *GeoForschungsZentrum Potsdam, Section 3.3, Telegrafenberg, D-14473 Potsdam, Germany*

Accepted 2008 June 23. Received 2008 June 21; in original form 2007 December 14

SUMMARY

Three up to 520-cm-long sediment cores from Hoya San Nicolas in Guanajuato, Mexico, were analysed for various magnetic properties in order to better define a palaeomagnetic secular curve for Central Mexico. The results—magnetic susceptibility, hysteresis cycles, anhysteretic and isothermal remanent magnetization—suggest that the remanent magnetization of the sediments is controlled by ferrimagnetic minerals (pseudo-single domain magnetite), which are suitable recorders of the geomagnetic field. The age–depth model indicates average deposition rates of 0.32 (interval 146–198 cm) and 0.45 mm yr^{-1} (interval 200–520 cm) and a basal age of about 11 600 calibrated years BP (cal. yr BP).

We used magnetic susceptibility and natural remanent magnetization to correlate the three cores. A composite palaeomagnetic secular variation (SV) record was obtained from the cores with a stretching and stacking process, and a chronology established with accelerator mass spectrometer dates on microscopic charcoal and stratigraphic correlations with other well dated Holocene records from Mexico and Guatemala. The declination and inclination results show oscillatory behaviour varying in a narrow range, although a distinctive directional swing is evident between 9060 and 9810 cal. yr BP. The San Nicolas palaeomagnetic SV curve is similar to palaeomagnetic master curves from Europe and North America, in shape, occurrence and synchronicity of directional features, especially with respect to inclination.

Key words: Environmental magnetism; Palaeomagnetic secular variation; Rock and mineral magnetism.

1 INTRODUCTION

It is well known that under favourable conditions, lake sediments can record the geomagnetic secular variation (SV) by means of a depositional or post-depositional remanent magnetization. Furthermore, if the sedimentation rate is high these sedimentary records represent high-resolution archives of the temporal variation of the earth's magnetic field.

Since the 1970s, numerous high-resolution lake sediment records of palaeomagnetic SV have been published; for example, Turner & Thompson (1979, 1981), Creer & Tucholka (1982a,b), Creer *et al.* (1983a,b), Lund & Baneerje (1985), Gogorza *et al.* (1999), Irurzun *et al.* (2006), Snowball *et al.* (2007). The coverage is particularly good for most of North America but relatively few reliable data are available for Mexico (Liddicoat *et al.* 1979; Ortega-Guerrero 1992; Ortega-Guerrero & Urrutia-Fucugauchi 1997). Furthermore, the Mexican data are often difficult to interpret because of problems related to the depositional environment, age models and the accuracy of palaeomagnetic measurement (Böhnel & Molina-Garza 2002). For example, Liddicoat *et al.* (1979) carried out their study on a former shoreline of a lake, and their sediment core contained numerous air-fall tephra layers. Ortega-Guerrero (1992) and Ortega-Guerrero & Urrutia-Fucugauchi (1997) have produced the only available SV data from lake sediments in Mexico; however, their record is compromised by an ambiguous age model, and their samples were only demagnetized at one step (Böhnel & Molina-Garza 2002). New palaeomagnetic data, are therefore, needed if a reliable SV curve is developed for central Mexico. The present study is the first part of a systematic effort to develop such a curve. The study site is La Hoya de San Nicolas, a maar crater located near the town of Valle de Santiago in Guanajuato, Mexico (Fig. 1).

2 STUDY AREA

Valle de Santiago (Guanajuato state, Mexico) is located in the central part of the Trans-Mexican Volcanic Belt (Fig. 1), an active

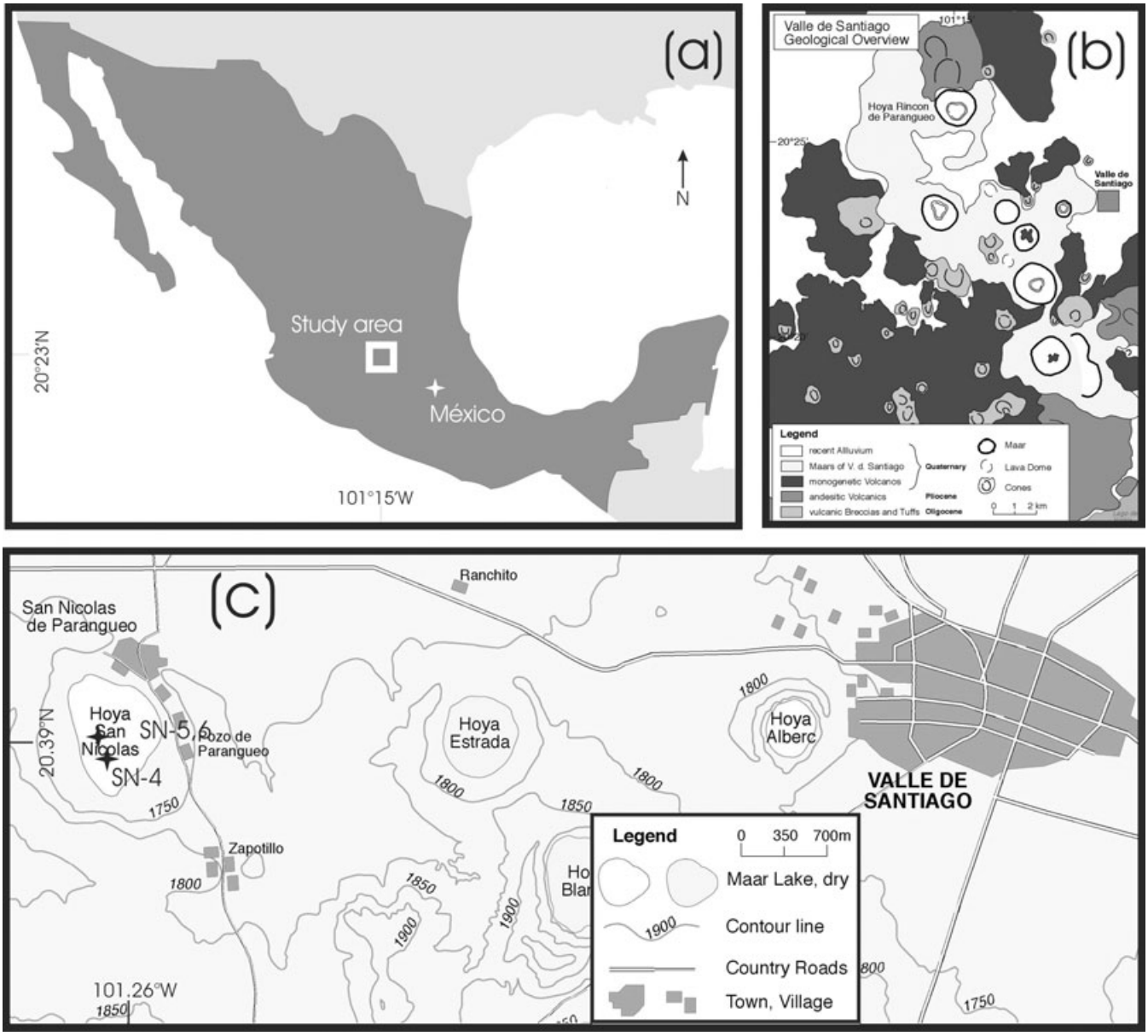

Figure 1. Map of (a) the study area in Mexico, (b) geological description and (c) Valle Santiago and the studied maar lake, Hoya San Nicolas.

volcanic arc related to the subduction of the Cocos/Rivera plate during the last 17 Ma (Ferrari *et al.* 2000). The study area includes a series of crater or maar lakes on the flood plain of the Lerma River at an altitude of about 1800 m above sea level (a.s.l.). According to Alcocer *et al.* (2000), there are nearly 30 craters in the Valle Santiago area, but only a few of them are deep enough to reach the water table and contain lakes. Before recent ground water exploitation caused a lowering of the water table, seven maars contained lakes: Hoya Alberca, Hoya Alvarez, Hoya Blanca, Hoya Estrada, Hoya La Cintura, Hoya Rincon de Parangueo and Hoya San Nicolas (Fig. 1b). The geology of the area is dominated by Oligocene to Quaternary basaltic lava flows, breccias, and tuffs (Murphy 1982). Murphy (1982) determined K-Ar dates of units associated with some of the maars that may be considered as maximum ages, being 0.073 $\pm$ 0.024 Ma for Hoya Alberca, 0.27 $\pm$ 0.20 Ma for Hoya Estrada, 0.38 $\pm$ 0.32 Ma for Hoya Cintura and 1.175 $\pm$ 0.166 Ma for Hoya San Nicolas.

Due to falling water levels during the last 40–50 yr, sediments in several of the maars are now easily accessible. Two of the maars contain shallow lakes while the rest have already dried out. Hoya San Nicolas desiccated in the 1970s, although the former lake floor is usually flooded during the rainy season.

3 MATERIAL AND METHODS

3.1 Field and sampling

The three cores reported on here, SN-4, SN-5 and SN-6, were recovered from the exposed lake bed at Hoya de San Nicolas (Lat. 20.39°N; Long. 101.26°W, elevation of ~1750 m a.s.l.). The former lake had a maximum area of ~0.5 km^2 (Fig. 1c). The cores were raised from the central part of the lake floor, with distances between them of 50–100 and 3 m, respectively. Each core was recovered by pushing a 6-m-long PVC tube into the sediment. The tubes were

fitted with pistons to minimize sediment loss, and the core length was ∼5 m for each core. All three cores were azimuthally oriented before extraction. Previous experience had shown that 8 cm diameter PVC-tubes fitted with a piston allow relatively undisturbed recovery of up to 5.5-m-long cores.

The cores were transported to the laboratory and stored at 4–7 °C. The PVC-tubes were opened using an electric saw attached to a linear slide mechanism and the cores split in half by pulling a thin wire through the sediment. The freshly exposed surface of one half core was then photographed and described stratigraphically. High-resolution magnetic susceptibility measurements were also made on the same half core. One half-core was stored as archive in a cold room; the other subsampled the following way. The half-core was placed with its plane surface on a table with 19 mm high guides. With a thin wire, the upper section was cut-off and packed in 5 cm parts in evacuated plastic bags for pollen and geochemical analyses (the results of which will be presented elsewhere). The remaining slab was subsampled using (8 cm^3) plastic cubes pushed into the central part of the slab, and by two u-channel profiles, which were pushed on both sides of the plastic cubes into the sediment. In this way we obtained from each half-core discrete samples every 21–23 mm, as well as two parallel continuous u-channel samples. Most results are based on the discrete samples, as the response function of the magnetometer used had a half-width of more than 10 cm and thus a much reduced spatial resolution compared to discrete samples. Between experiments, all samples were stored at ∼5°C to reduce as far as possible water loss and alterations.

3.2 Core chronology

Core chronology was established by accelerator mass spectrometer (AMS) dating of microscopic charcoal and by stratigraphic correlation with other well dated Holocene records from Mexico and Guatemala. Four samples of microscopic charcoal were submitted to Lawrence Livermore National Laboratory CAMS and one sample to Woods Hole Oceanographic Institution NOSAMS. Each sample consisted of concentrated microscopic charcoal hand picked from a >125 μm sieved fraction. Sample preparation procedures are detailed in Park (2005). Calibrated age ranges were determined with the CALIB 4.4 program (Stuiver *et al.* 1998).

3.3 Magnetic methods

Magnetic susceptibility was measured with a high resolution scanning system (Nowaczyk 2001) based on a Bartington MS2 instrument with high-resolution sensor MS2E, providing a step resolution of 1 mm and a sensor spatial resolution of 4 mm. Both half-cores were measured and data were later averaged.

All measurements were carried out in the palaeomagnetic laboratory of the GeoForschungsZentrum Potsdam. Low-field magnetic susceptibility and its anisotropy were measured with a KLY-3 instrument from AGICO. For remanence measurements, a 2G-Enterprises long-core rock-magnetometer with attached alternating field (AF) demagnetizer was used (max. field 150 mT). This could hold either one u-channel <1.5 m long or up to eight discrete samples at a time. IRM acquisition was done with a 2G-Enterprises pulsmagnetizer, and the IRM produced measured in a Molspin magnetometer. ARM acquisition was done with a 2G-Enterprises single-axis AF demagnetizer.

After measurement of the magnetic susceptibility, NRM was measured and stepwise AF demagnetized with the 2G system. Then an ARM was produced in the samples and demagnetized in several steps. Next, IRM acquisition was carried out in detail for every tenth sample, followed by backfield demagnetization. Samples in between were exposed only to the highest field used here of 2 T, then to a backfield of −0.3 T for calculating the *S*-ratio.

From each discrete sample, a small amount of material was used to measure magnetic hysteresis loops in fields between −1 and 1 T at room temperature using a Princeton Measurement Corporation Micromag 2900 AGM system equipped with a 2.2 T magnet. Before the experiments, the material was dried and weighed to allow for calculation of mass-corrected hysteresis parameters.

Selected samples were studied in a Petersen Instruments VFTB magnetic balance to produce thermomagnetic curves. The inducing field chosen was ∼0.5 T, and ramp-rates during heating and cooling were 30–40°C min^{-1}. Argon was used for flushing the sample space.

3.4 Macroscopic description

The San Nicolas cores show little vertical variation in visual stratigraphy. The sediments are mostly fine silt and clay (Fig. 2). In the basal sections, 520 cm to about 400 cm, the sediments were alternately dark grey and blue in colour prior to exposure after which they changed to olive. From about 400 cm to about 200 cm the oxidized sediments are dark brown in colour. At about 300 cm there is a change from deposition of very fine sand, coarse silt and medium silt (∼10, 40 and 40 per cent, respectively) below this level, to coarse silt, medium silt, fine silt and clay (30, 30, 30, 5 per cent, respectively) above this level. Between 200 and 180 cm there are lenses of medium sand and small calcite concretions. The upper part of the core is again mostly fine silt and dark greyish brown in colour, with a narrow laminated section between 165 and 155 cm and evidence of desiccation at about 60 cm. No molluscs were observed in the cores although ostracodes are abundant at about 125 cm. Five tephra layers are present at 111, 179, 205, 285 and 315 cm, with thickness of 1–3 mm.

4 RESULTS AND DISCUSSION

4.1 Age model

The results of AMS radiocarbon dates with 2σ errors, the calibrated age ranges at 95.4 per cent confidence limits (2σ) and the median are listed in Table 1. Furthermore, three cross-correlated dates from Preboreal events (PBE) evident in geochemistry data for core SN-6 are included in the age model and listed with corresponding age ranges in Table 1. These PBE which are evident as short periods of drier climate in the San Nicolas core have been identified in marine cores from the Gulf of Mexico (Aharon 2003) and in lake cores from Central America (Hillesheim *et al.* 2005); these events are interpreted to be glacial meltwater pulses during the last deglaciation. In particular, the dates for events PBE2, PBE3 and PBE4 reported in Hillesheim *et al.* (2005) are the most reliable for this study because they are based on wood. The details of the geochemistry/PBE correlation are discussed in more detail in the section dealing with sediment chemistry and rock magnetism.

All age data with 2σ errors and the age model are shown in Fig. 3. The age model is based upon two linear regressions for the depth intervals 146–198 and 200–520 cm.

$$\text{cal. age} = 31.0 \times \text{depth} - 2522 \quad (1)$$

$$\text{cal. age} = 22.2 \times \text{depth} + 81.7 \quad (R = 0.986;\ p = 0.002). \quad (2)$$

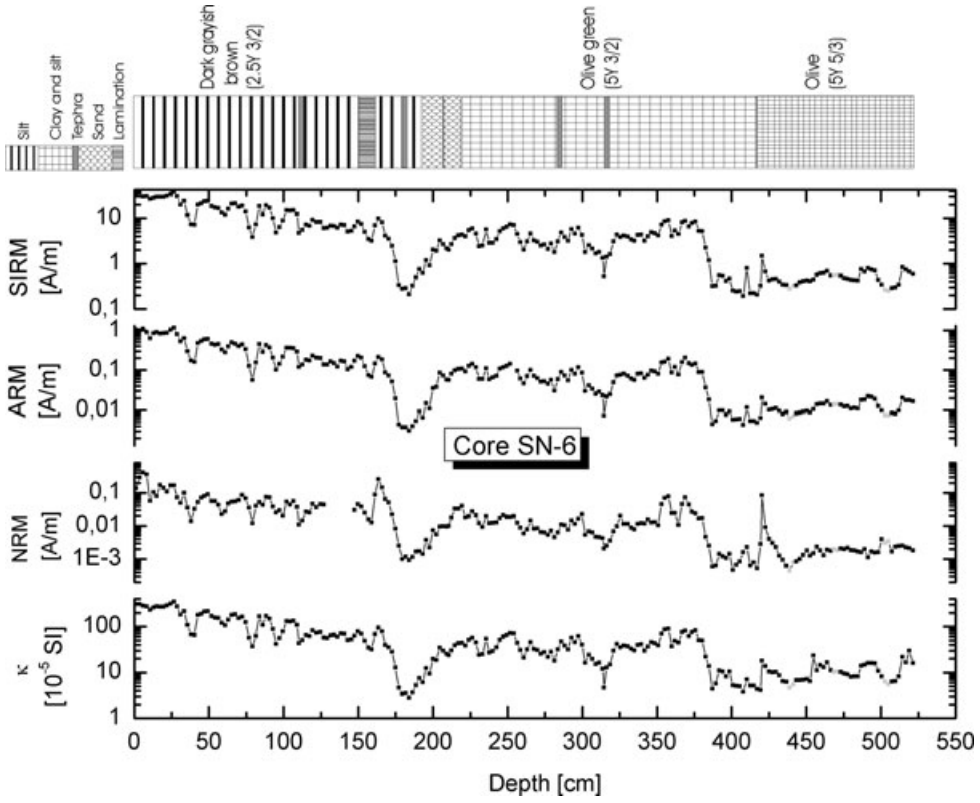

Figure 2. Concentration dependent magnetic parameters and simplified lithology of the master core SN-6.

Table 1. AMS radiocarbon dates, calibrated ages ranges at 95.4 per cent confidence limits (2σ) and the median calibrated ages from the master core SN-6.

Core	Material	Preboreal event[a]	Depth (cm)	Laboratory number	Age (^{14}C yr BP)	δ^{13}C (‰)	2σ cal. age range (cal. yr BP)	Cal. age (cal. yr BP)
SN-6	Charcoal	–	147.5	CAMS-102239	2070 ± 110	−16	1820–2330	2050[b]
SN-6	Charcoal	–	197.5	CAMS-102240	3350 ± 140	−16	3270–3970	3600[b]
SN-6	Charcoal	–	237.5	CAMS-102241	4640 ± 100	−16	5050–5590	5360[b]
SN-6	Charcoal	–	382.0	OS-46420	7390 ± 75	−16	8040–8360	8220[b]
PI 8-VI-02 11A	–	PBE4	439.5	–	–	–	10 310–10 460	10 400[a]
PI 8-VI-02 11A	–	PBE3	469.5	–	–	–	10 660–10 800	10 700[a]
PI 8-VI-02 11A	–	PBE2	504.5	–	–	–	10 880–11 010	10 900[a]

[a]Dates from cross-correlation using Preboreal event (PBE) identified in Hillesheim *et al.* (2005).
[b]Dates were calibrated with the intcal98.14c data set (Stuiver *et al.* 1998).

The age–depth conversion was carried out after a previous depth interpolation (at 2 cm) for the stacking process. The sedimentation rates are about 0.32 mm yr^{-1} (146–198 cm) and 0.45 mm yr^{-1} (200–520 cm); this difference together with geochemistry and palynological arguments (Park 2005) suggest that there may be a hiatus at 200 cm, representing a gap of ∼900 yr [from about 4500 to 3600 calibrated years BP (cal yr BP)].

The basal age of about 11 600 cal. yr BP predicted by the age model agrees with a basal date of 12 500 ± 1020 cal. yr BP reported in an earlier pollen study of a 530 cm core from San Nicolas by Brown (1984).

4.2 Rock-magnetic studies

Rock-magnetic data are available for all cores, but only results for the master core SN-6 are shown; the data from the other cores show essentially the same features.

The main magnetic carriers are ferrimagnetic minerals as can be inferred from *S*-ratio, MDF and H_{CR} parameters (Fig. 4). Magnetomineralogy seems rather uniform down-core, except in two sections (170–210 and 385–520 cm) where changes in carriers should be considered. Magnetite-like carriers are the responsible for the remanence data, for example, values of H_{CR} (about 33 mT, see Fig. 4) belong to the range of (titano)magnetite (Peters & Dekkers 2003). Parameter variations in the above mentioned sections lead to relative changes in magnetic mineralogy; the drop off of *S*-ratio (from about 0.98 to 0.94) and the increase of H_{CR} (from 32.7 to 46.1 mT) are coherent between them. In Fig. 5(a), magnetic mineralogy can be observed as two data grouping of samples belonging to 0–385 cm (upper left-hand side) and to 385–520 cm (lower right-hand side).

According to these parameters, two possibilities can be taken into account to explain differences in magnetic carriers at 170–210 and 385–520 cm. One involves variations of oxidation state and/or

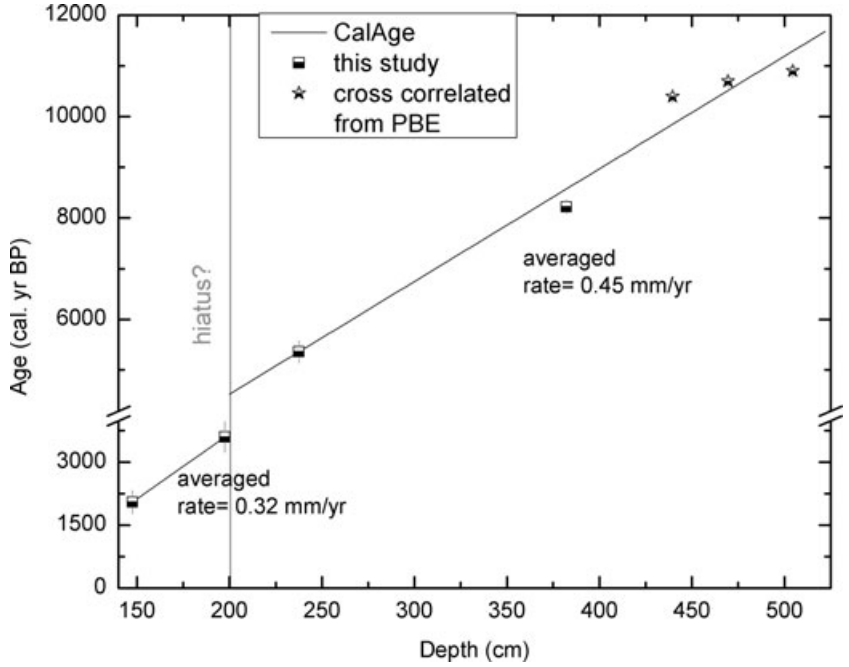

Figure 3. Calibrated radiocarbon dates and the age model.

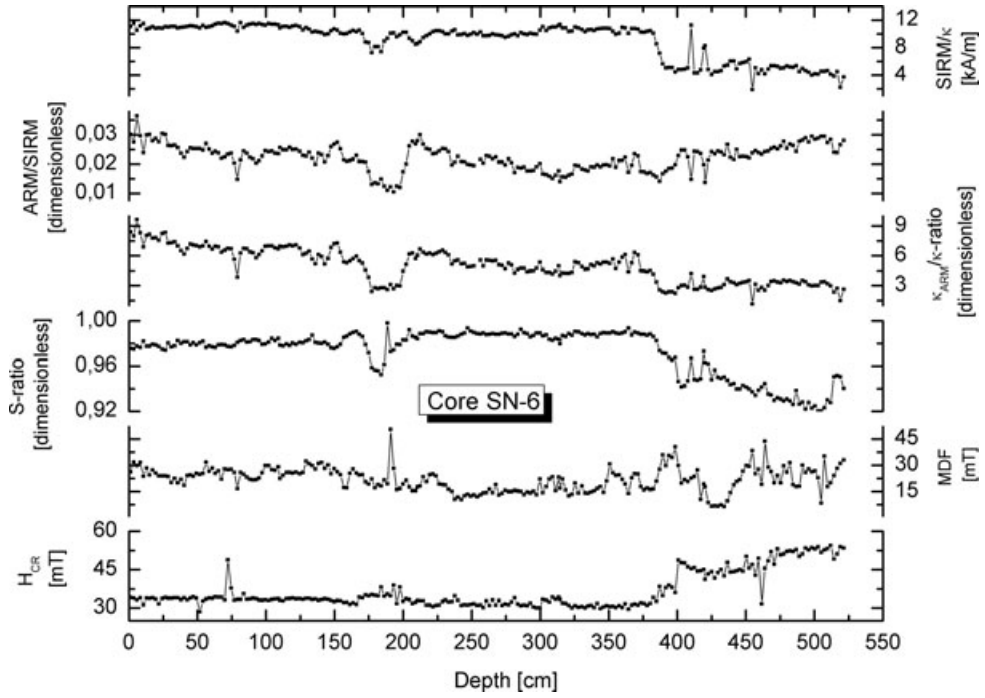

Figure 4. Down-core variation of rock-magnetic parameters of the master core SN-6.

grain size of magnetite, the other, more plausible one, considers that another mineral, such as hematite and/or goethite, is contributing to increase the coercivity remanence.

The latter hypothesis is supported from methods to separate magnetic component in IRM acquisition curves (e.g. Stockhausen 1998; Kruiver *et al.* 2001). Although the IRM acquisition curves mainly indicate the presence of only one carrier and saturates in fields <300 mT, results from IRM separation studies (not shown) yielded one magnetic component (e.g. contribution1 = 100 per cent, $H_{1/2}$ = 44.7 mT) at about 330 cm; and two components (e.g. contribution1 = 93.4 per cent, $H_{1/2}$ = 53.7 mT; contribution2 = 6.6 per cent; $H_{1/2}$ = 199.5 mT) between 385 and 520 cm.

Therefore, (titano)magnetite is considered as the main magnetic carrier along the core, and the presence of a subordinate hard magnetic carrier is suggested below 385 cm. For the interval 170–210 very low ARM/SIRM ratios and lack of frequency dependency of magnetic susceptibility indicate primarily a marked reduction in contributions from very fine particles—single domain (SD) or

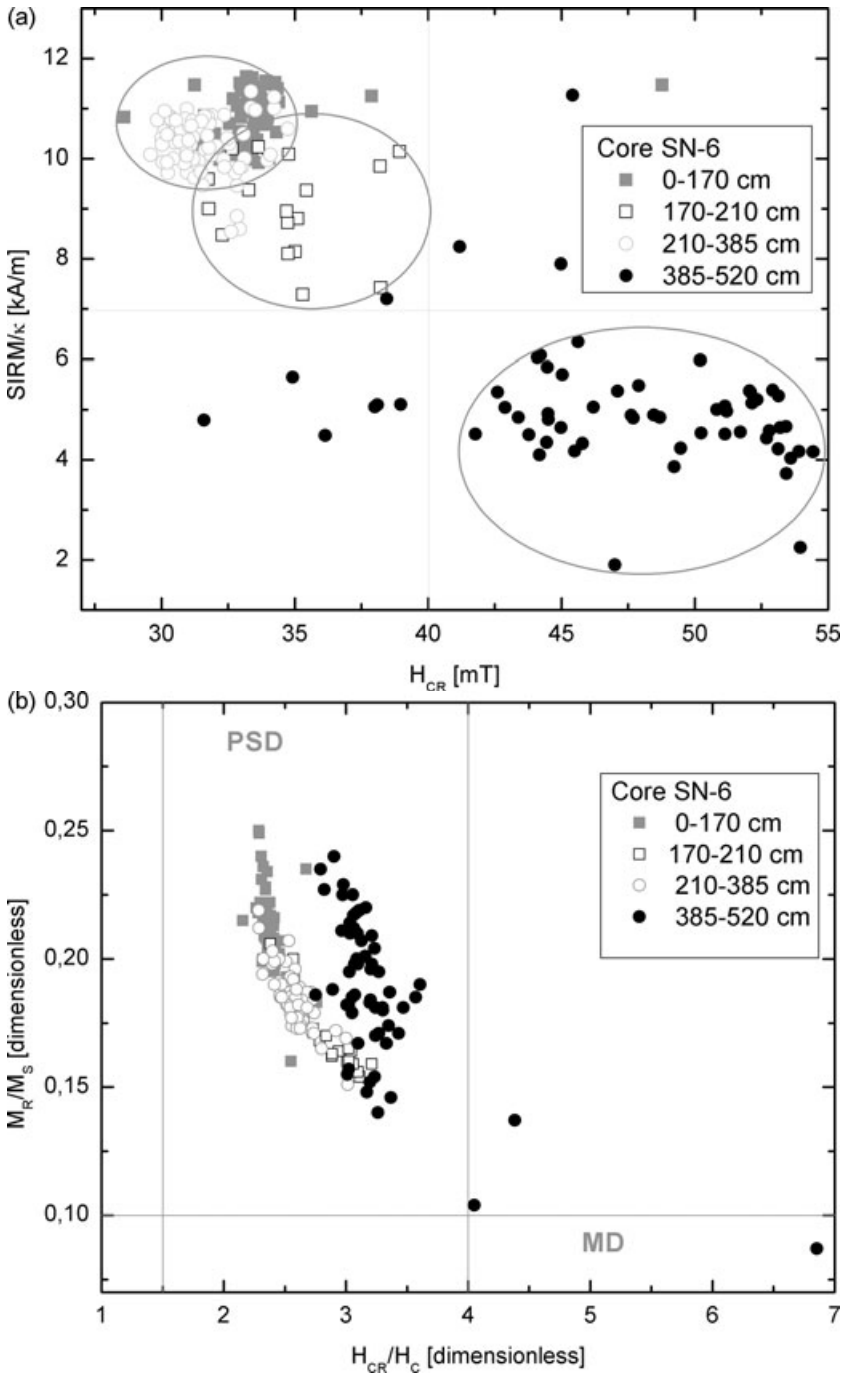

Figure 5. Magnetic results of the master core SN-6: (a) biplot SIRM/κ versus H_{CR} revealing magnetic mineralogy; (b) day biplot of M_R/M_S versus H_{CR}/H_C indicating magnetic domain state.

pseudo-single domain (PSD)—of (titano)magnetite. Notice that this reduction is not observed below 385.

Measurements of temperature dependence of κ (κ–T curves) are not displayed here. However, from this study, the T_C (about 585°C) suggests that magnetite is the main magnetic carrier, supporting the above conclusions from other magnetic measurements. The heating and cooling curves show a similar pattern, showing a reversible behaviour, and therefore, neoformation of magnetic minerals is not expected.

The magnetic grain size dependent parameters (κ_{ARM}/κ-ratio, ARM/SIRM and SIRM/κ) show a similar trend as can be observed in Fig. 4. SIRM/κ variation may not necessarily reflect grain size variation (Maher 1986) because magnetic mineralogy seems not to be uniform down-core. Changes in the κ_{ARM}/κ-ratio indicate the occurrence of coarser magnetic grain sizes between 170–210 and 385–520 cm, which is a highly grain size dependent parameter for magnetite (Peters & Dekkers 2003). Therefore, a combination of magnetic mineralogy and grain size changes could be possible, and both should be taken into account.

Hysteresis parameters were determined from the hysteresis loops, and two useful ratios, that is, M_{RS}/M_S and H_{CR}/H_C, were also calculated and plotted against each other in the Day plot (Day *et al.*

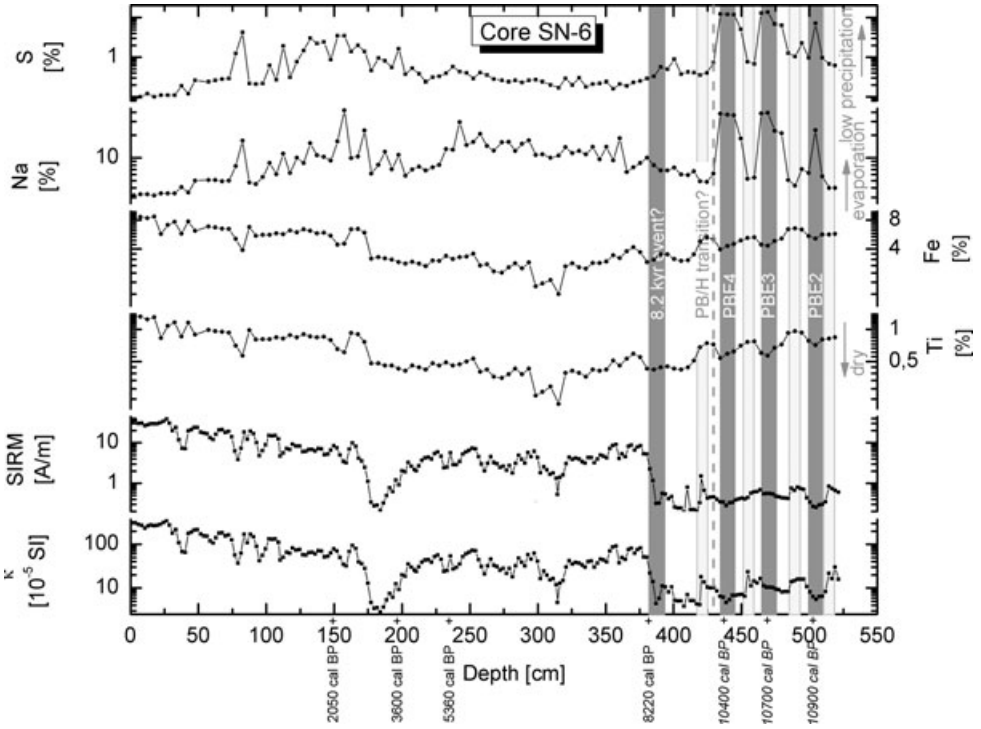

Figure 6. Down-core variation of erosional and evaporative indicators and magnetic parameters for the master core SN-6.

1977). As can be observed in Fig. 5(b), most of the samples are well grouped in the PSD zone. However, this should be considered with caution, as such data could also be produced by the combination of SD and multidomain (MD) grains according to the above discussion of other grain size dependent parameters.

On the other hand, concentration dependent magnetic parameters, such as κ, NRM, ARM and SIRM, show a relative high variability along the sequence (Fig. 2). Such a variability as consequence of magnetic mineral concentration can reflect environmental and climatic-induced changes and the human influence during different periods. These conclusions were also discussed in Park (2005), which was obtained from palynological and geochemical studies.

These concentration dependent parameters are coherent between each other, showing two intervals of low concentration, from about 170 to 210 cm and from 385 to 520 cm. Magnetic concentration decreases from the upper to the lower section; as can be seen in Fig. 2, the highest values are observed between 0 and 170 cm.

4.3 Sediment chemistry and Rock-magnetic parameters

As detailed in Park (2005), XRF studies were carried out on 103 samples of the core SN-6, obtaining data for 11 common elements (oxides) and 25 trace elements. The details of these results will be presented elsewhere (Park *et al.* in preparation). Here, we present data of four elements—Ti (TiO_2), Fe (Fe_2O_3), Na (Na_2O) and S (SO_3)—and compare them with two magnetic parameters (magnetic susceptibility and SIRM). The down-core variation of the selected oxides and magnetic parameters are shown in Fig. 6. Ti and Fe contents are usually interpreted as erosional indicators (Bradbury 2000), and Na and S are interpreted as evaporation indicators, being indexes of reduced precipitation and increased evaporation.

The lowermost section of the core (420–520 cm) is of particular interest for this study, showing a short term variation of the oxides (Park 2005) as well as of the magnetic parameters. In Fig. 6 three prominent peaks are visible for Na and S which correlate with lows of Ti, Fe and κ and SIRM. These peaks and lows are marked by shaded bands around 440, 470 and 505 cm and are interpreted as dry phases with increased evaporation. Comparing our data with Na and S variations from Lake Petén Itzá (Hillesheim *et al.* 2005) and Cariaco Basin (Haug *et al.* 2001), these dry phases may correspond to the three Preboreal events PBE4, PBE3 and PBE2. Two additional events corresponding to the Preboreal/Holocene transition and the 8.2 kyr event may be present in core SN-6 but they are not as well constrained. Between the mentioned dry phases, relative lows are observed for Na and S, and relative highs for Ti, Fe, SIRM and κ. These variations are not as well expressed as the previously mentioned ones, but they seem to suggest more humid conditions alternating with the dry phases. Such climatic oscillations have been proposed by Hillesheim *et al.* (2005) who suggested that episodic meltwater discharge into the Gulf of Mexico during the Preboreal was sufficient to cause regional changes of the evaporation/precipitation ratio.

For levels between 420 and 350 cm Park (2005) suggested, based on geochemical and palynological proxies, a period of more humid climate, which shifted to drier climate going upwards towards 180 cm. The uppermost 180 cm are characterized by a notable increase of erosional indicators, which together with the occurrence of *Zea* pollen and other disturbance taxa is interpreted mostly due to human disturbance.

4.4 Palaeomagnetic studies

4.4.1 Palaeomagnetic stability

Stability studies were carried out using AF demagnetization studies; some selected samples were studied using increasing AF of 5, 10, 15, 20, 30, 40, 50, 60, 80 and 100 mT. The MDF varied from

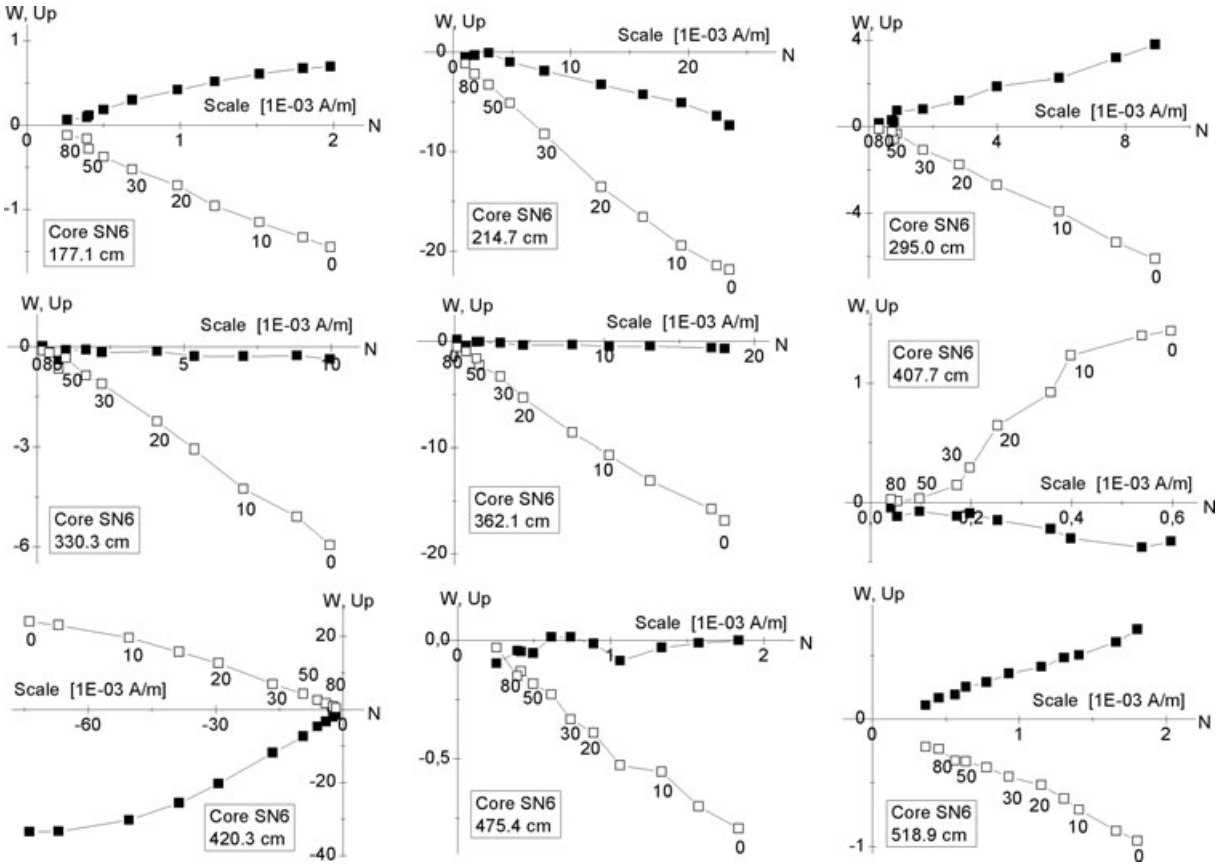

Figure 7. Examples of AF demagnetization behaviour of samples from the master core SN-6. Orthogonal demagnetization plots, Zijderveld diagrams, solid (open) symbols are projections onto the horizontal (vertical) plane.

6.5 to 50.3 mT (Fig. 4), but the mean is 21.9 mT with a small standard deviation (*S.D.*) of 6.8 mT. This result is in agreement to the predominance of soft magnetic carriers that was discussed above.

Demagnetization data were plotted on orthogonal plots or Zijderveld diagrams (Zijderveld 1967). As seen from Zijderveld diagrams in selected samples (Fig. 7), progressive AF demagnetization of discrete samples reveals that the natural remanent magnetization (NRM) is nearly single component without an important viscous overprint, as well as it has mainly a north to northwest and down directed component. Small viscous components were observed in some samples but easily removed by 15 mT peak AF.

The direction of characteristic remanent magnetization was determined by principal component analysis (Kirschvink 1980). Typically, 4–6 steps in the demagnetization interval 20–60 mT were used to fit lines, based on the Zijderveld diagrams.

4.4.2 Stretching process

Down-core variation of κ for cores SN4, SN-5 and SN-6 is shown in Fig. 8 and used to correlate these cores, providing a lithostratigraphic connection between them. This correlation is made on the reasonable assumption that sediments were deposited in calm water and cores are parallel. Core SN-6 was chosen as the master core, and depth scales of cores SN-4 and SN-5 were adjusted to core SN-6 using 25 tie lines. Although most of these tie lines were defined from κ logs alone (Fig. 8), some were defined by the additional use of the NRM intensity variation. Between tie lines, linear interpolation was used to transform depths to a common scale for comparison of the palaeomagnetic record of the individual cores.

After this stretching process was performed, NRM intensity and directions were plotted using the adjusted depth scale or stretched depth (see Figs 9a–c). NRM intensity shows in general a good between-core alignment of peaks and lows (Fig. 9a), except for the uppermost ∼170 cm (marked in Fig. 9 with shaded background). As already noted from the κ logs, this section seems to be affected by human influences (e.g. farming around and within the maar lake basin). In particular, the high *Zea* (cultivated maize) and Amaranthaceae percentages, as well as the increase of erosional indicators (Al_2O_3, Fe_2O and TiO_2) are clear evidence of more or less continuous human disturbance (Park 2005). Data from this section (0–170 cm) were not considered for the SV curve.

Below 170 cm, directional data (*I* and *D*) from the available cores show similar trends, in particular, correspondence among the inclination logs is clear. Such a correspondence indicates a magnetostratigraphic correlation, proving that lithostratigraphic connections have chronostratigraphic meaning.

Inclination values oscillate around the geocentric axial dipole (GAD) at this site, which is about 34.5°. Statistics for each core in these sections reveal that inclination varies in a moderate range: mean (and *S.D.*) values are 39.0° (14.6°) for core SN-4, 33.6° (13.4°) for the mastercore SN-6, and 38.7° (11.5°) for core SN-5.

Although declination patterns show similarities among them, the *D* values of core SN-4 seem to decrease systematically downward (Fig. 9b), which is also indicated by the mean (and *S.D.*) value

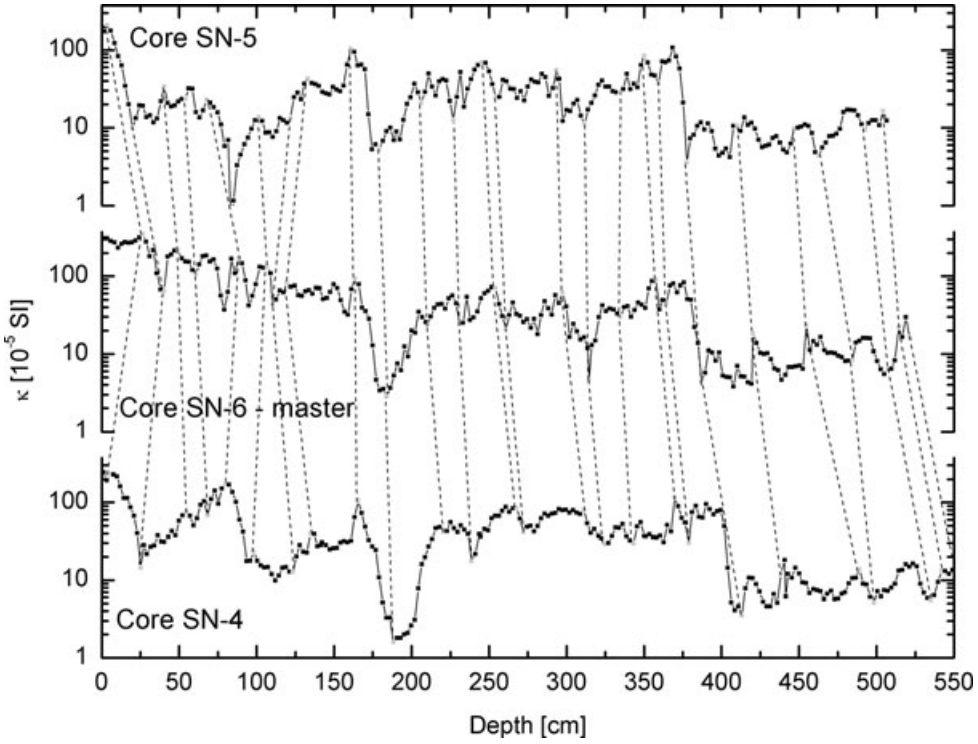

Figure 8. Down-core variations of magnetic susceptibility and correlation tie lines between cores SN-4, SN-5 and the master core SN-6 are shown.

of −33.4° (27.0°), while this is close to zero for core SN-6, 0.6° (20.7°) and core SN-5, −0.8° (23.2°). Thus it seems to be evident that sediments from core SN-4 have experienced a rotation within the PVC tube that increases with depth. This rotation seems to be systematic because most declination peaks and lows still agree with those from the other cores, for example, the pronounced swing at about 420 cm. Therefore, data from this core were not used for the stacking process.

It is worth mentioning that an important swing in both directional data, I and D, occurs between 400 and 425 cm, and that this swing is observed in all cores showing simultaneity and consistency of the palaeomagnetic record. Changes are particularly strong in the inclination reaching even negative values (Fig. 9c) and are not accompanied by significant variation in rock magnetic parameters as κ, ARM and SIRM (see Fig. 2).

4.4.3 Stacking process

As in most of palaeomagnetic studies in lake sediments, the stacking procedure is aimed at removing the spurious data exhibited by individual records and enhancing the signal/noise ratio. Hence, the stacked record is often found to show fewer fine details than the individual records (Creer & Tucholka 1982b). For each core a depth interpolation at 2 cm increments was applied, and then the Fisher method (Fisher 1953) was used in order to obtain composite records. These composite I and D results and their corresponding errors (δ, angular standard deviation), are shown in Fig. 10. According to Butler (2004), the δ (eq. 3) is used as a measure of angular dispersion,

$$\delta = \cos^{-1}(R/N), \tag{3}$$

where R is the length of the vector sum of the individual unit vectors and N is the number of data.

Both curves show clear resemblance with the curves of individual cores (Figs 9b and c), but as a consequence of the stacking process they are smoother. Simultaneous changes in I and D data are visible at 15 specific depth levels marked in Fig. 10 by vertical lines or shaded bands and thus define the most important SV features for this lake.

4.5 The SV curve and comparison with other available data

To obtain a SV curve, depth scales were transformed into time-series using the proposed age model (see above), which allow the stacked results to be plotted versus calibrated years BP (Fig. 11). The timescale spans about 9000 yr, from 2800 to 11 600 cal. yr BP.

An oscillatory behaviour around 0° in declination and 34.5° in inclination is observed from the SV curve (Fig. 11), and several changes in D and I occurred simultaneously with the most pronounced one at about 9060–9810 cal. yr BP. Here directions show a significant swing within a short period of about 800 yr (Fig. 11), with declination changes from about 0° to 87.7°; inclination reaches negative values, varying from about the GAD inclination (34.5°) to −19.7°. These directional results suggest an interesting anomaly between 9060 and 9810 cal. yr BP that could be interpreted as a geomagnetic excursion or even a very short reversal record of the geomagnetic field. Although this directional anomaly was recorded in all cores without showing important changes in rock magnetic parameters, its interpretation should be treated cautiously and further data are required to validate the excursion's existence.

4.5.1 Lava flow data

Palaeomagnetic data are available from recent volcanic rocks (Gonzalez *et al.* 1997; Vlag *et al.* 2000; Böhnel & Molina-Garza

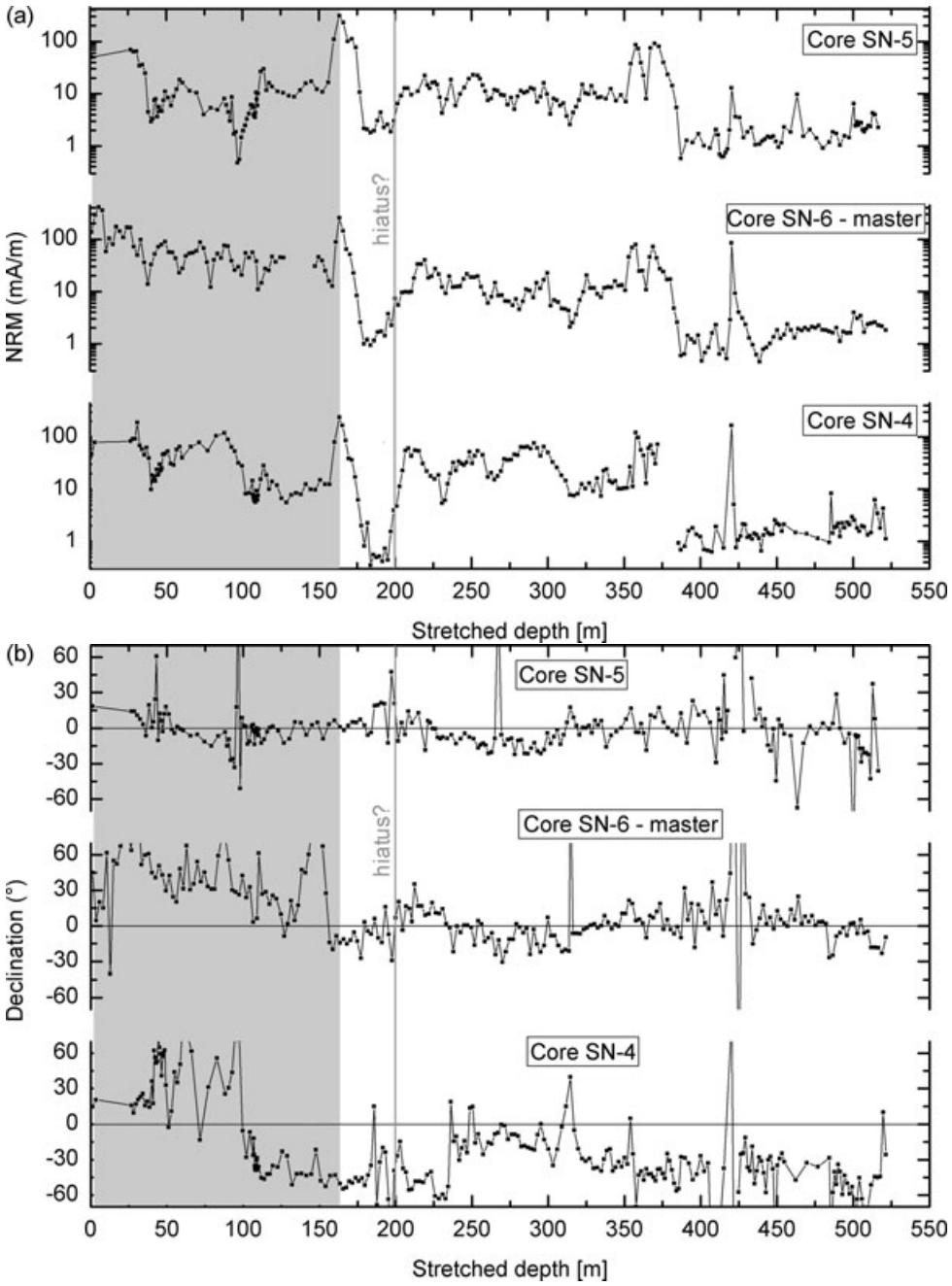

Figure 9. Palaeomagnetic results versus stretched depth of all cores. Possible influenced and disturbed sediments sections have been marked with grey boxes. (a) NRM intensity, (b) declination (c) inclination and the GAD value (34.5°).

2002; Barajas-Gea & Rodriguez-Vargas 2005), but data are spread unevenly over the period of interest here. The dates in radiocarbon ages BP in these mentioned articles were uncalibrated; for comparison with the lake sediment data, calibrated ages were calculated by applying the CALIB 5.0 program (Stuiver *et al.* 2005). These data and the SV curve (this study) are shown in Fig. 11. Inclination and declination results show a similar trend during the first period, back to 5500 cal. yr BP.

Prior to 9450 cal. yr BP, data differ partially, fitting very well in inclination at 9460 cal. yr BP, and at 10 370 cal. yr BP, as well as in declination and inclination at the basal section, if the age error for these lava data is considered. There is a need for lava flow data between 5400 and 9400 cal. yr BP, especially around 8500–9400 cal. yr BP to corroborate the anomalous geomagnetic behaviour observed.

4.5.2 SV master curves from other lake sediments

The obtained SV curve for Lake San Nicolas was compared with other curves from the northern hemisphere (Turner & Thompson 1982; Creer & Tucholka 1982a; Lund & Baneerje 1985; Verosub *et al.* 1986; Lund *et al.* 1988; Ortega-Guerrero 1992; Peng & King 1992; Snowball *et al.* 2007). Since the SV curve constitutes a preliminary result in Mexico and was constructed using only data from the San Nicolas maar, a comparison with other SV master curves—based on data from several lakes in a region or country—

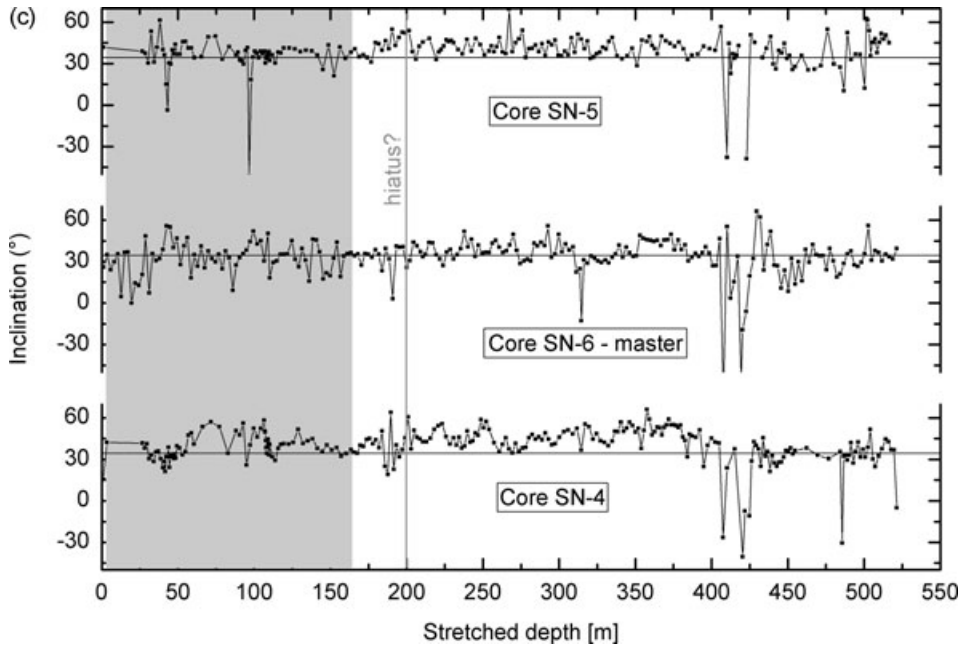

Figure 9. (*Continued*).

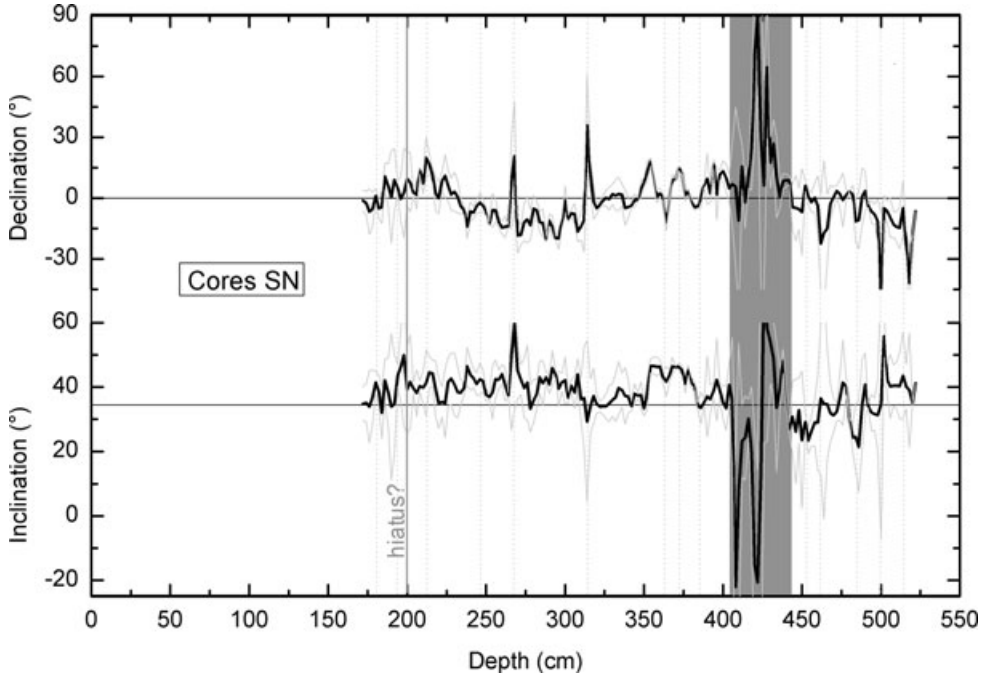

Figure 10. Composite records of data from cores SN. Stacked declination and inclination versus the adjusted depth.

may not be entirely appropriate because of the missing interlake smoothing and of the differing geographic position. However, the purpose of our comparison is to corroborate qualitatively if the main *D* and *I* features are observed in this study as well. The North America curves involve two regional master curves, one from the Great Lakes (USA, combined Lakes Huron, Superior, St Croix and Kylen Lakes; 43–48°N to 82–98°W) and the other one from the Western USA (combined Fish Lake and Mono Lake; 38–42°N to 119°W). Uncalibrated radiocarbon ages (as well as the Lake Waiau (Hawaii) and Lake Chalco, Mexico) were converted using the CALIB 5.0 program (Stuiver *et al.* 2005). From Europe, the UK (combined Lake Windemere, Llyn Geirionydd and Loch Lomond; 55°N–4°W) and Fennoscandia (Sweden and Finland, combined Lake Byestadsjön, Furskogstjärnet, Mötterudstjärnet, Sarsjön, Frängsjön, Alimmainen Savijärvi and Nautajärvi; 57–64°N to 12–25°E) master curves were also used for comparison. All mentioned curves, except Chalco data, were downloaded from the National Geophysical Data Center that hosts the IAGA sponsored Palaeomagnetic Databases, and from the supplementary data in Snowball *et al.* (2007).

Each directional dataset was smoothed (with ∼150–250 yr running windows) and then plotted in common variation range of inclination ($\Delta I = 40°$) and declination ($\Delta D = 90°$) for comparison purposes (see Fig. 12). The main features of the UK, Fennoscandia

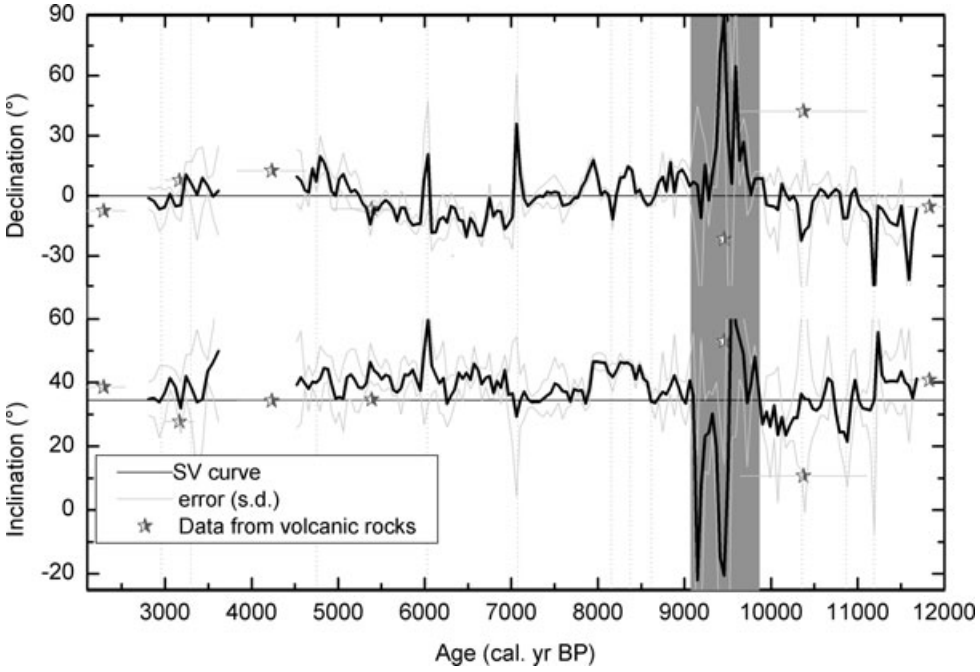

Figure 11. SV curve. Stacked *D* and *I* (and their corresponding *S.D.*) as function of cal. yr BP. Comparison of the obtained SV curve and data from lava flow (Gonzalez *et al.* 1997; Vlag *et al.* 2000; Böhnel & Molina-Garza 2002; Barajas-Gea & Rodriguez-Vargas 2005).

and Great Lakes curves were labelled according the corresponding nomenclatures used in the previous studies (Turner & Thompson 1981; Creer & Tucholka 1982b; Snowball *et al.* 2007) with Greek and Latin letters. As noted in Fig. 12, the main features observed in Lake San Nicolas (this study) were labelled according to the Great Lakes (USA) nomenclature.

There is a very good agreement of the main inclination features found in reliable SV master curves from the UK, Fennoscandia and Great Lakes. On the other hand, there is a poor agreement with *D* and *I* curves from Lake Waiau (Hawaii) where it is hard to identify the main features. Inclination variation of Lake Chalco (Mexico, Fig. 12) is higher and the pattern (details) of this curve differs from the others.

Nine inclination features were identified in the San Nicolas curve (see Fig. 12a), which are in agreement with European and North American features. As discussed in the literature (e.g. Creer & Tucholka 1982b; Snowball *et al.* 2007), there are shifts among features from curves attributed to an overall average annual westward drift, and possibly to systematic errors in the timescale for UK and North American data. However, there is a remarkable synchronicity and shape of some inclination features. Note, in particular, both characteristics for features *k*, *l* and *m* with features κ, λ and μ (UK) and *k*, *l* and *m* (Great Lakes), as well as feature *n* with and feature υ and features *f*, *h*, *i* with the corresponding from the Great Lakes. It is worth mentioning that the strong inclination swing found in this study (feature *m*) coincides very well with features μ and *m* (lows in inclination) from the UK and Great Lakes (USA) master curves, although in our study the inclination variation is much more important with $\sim 60^\circ$ change. Together, these data may indicate a short excursion (or period of abnormally strong SV) that expresses differently over the earth's surface.

Although there are differences between the San Nicolas and the other curves, note that all identified declination features (features *E*, *F*, *G*, *I*, *J* and *K*) are in agreement, but shifted, with the corresponding features from the Great Lakes (see Fig. 12b). Among the identified declination features, feature *J* is synchronous with feature *j* (Fennoscandia).

Creer & Tucholka (1982b) found a good correlation between the main inclination features from master SV curves of Europe and the Great Lakes, obtaining a phase shift of about 400 yr. that was interpreted in terms of an overall average annual westward drift of $\sim 0.24^\circ$; on the other hand, they also found that standing sources dominate the declination data. Therefore, Creer (1983) proposed that the SV could be modelled by a model that involves both standing and drifting parts of the non-dipole geomagnetic field. In a recent study, Snowball *et al.* (2007) have correlated the main features between European master SV curves (the UK and Fennoscandia curves), finding differences that can solely be explained by westward drift or higher components of the magnetic field, being necessary to take into account the lock-in depth of the NRM in different lake sediments and radiocarbon dating uncertainties as well. The latter problems have also been discussed by Vigliotti (2006), Ojala & Tiljander (2003) and other authors.

Nevertheless, as mentioned before, the purpose of our comparison is only qualitative, which is reasonable regarding that the San Nicolas SV curve is not considered a master SV curve for central Mexico. Therefore, we do not pretend to establish a precise correlation between features recorded here and in other parts of the world. We note however that, considering the given longitude differences of $\sim 10^\circ$ (San Nicolas–Great Lakes) and $\sim 97^\circ$ (San Nicolas–UK), the age differences between features μ and m could be interpreted in terms of an eastward drift, while features *i*, *k* and *l* are contemporary with ι, κ and λ. These differences probably reflect inaccuracies of the age model applied to the San Nicolas sediments.

5 CONCLUSIONS

Lake sediments from a new site in Mexico have been studied, and detailed rock-magnetic parameter analyses for these

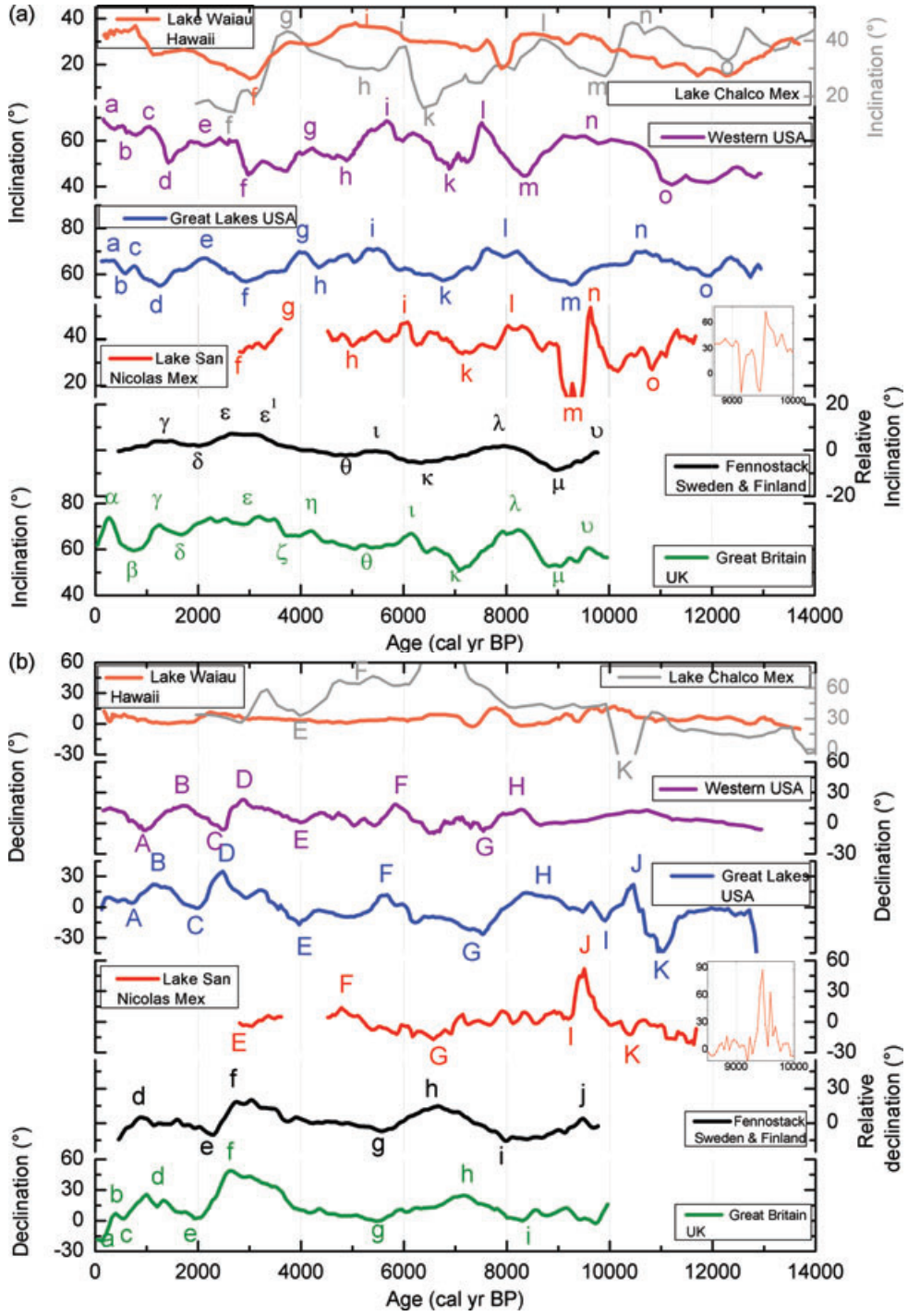

Figure 12. Comparison of SV curves (this study; Lake Waiau Hawaii; Lake Chalco Mexico) and master curves (UK; Sweden and Finland; Great Lakes USA; Western USA). (a) Inclination; (b) Declination. The North America and UK data were downloaded from the website of the National Geophysical Data Center (http://www.ngdc.noaa.gov/seg/geomag/paleo.shtml) that distribute the IAGA sponsored Paleomagnetic Databases. The Fennoscandia data was downloaded from Snowball *et al.* (2007).

sediments allow us to identify the main magnetic carriers. They are ferrimagnetic minerals, in particular, PSD magnetite that evidence a variable magnetic concentration along the core. Furthermore, the magnetic grain size increases down-core and subordinate antiferromagnetic minerals were also found below 385 cm.

It is worth mentioning that rock-magnetic parameters could also be used in future works as environmental proxies for climatically induced changes, for example, drought periods, in this study, Preboreal events (PBE) were identified; as well as human induced changes in recent period that correspond to the uppermost sediments (0–170 cm).

The main magnetic carriers are reliable recorders of the geomagnetic field, and the palaeomagnetic record is characterized by a strong and stable signal, hence good quality data for construction of a SV curve are expected from these lake sediments. The SV curve spans about 11 600 cal. yr BP and results of declination and

inclination show an oscillatory behaviour around 0° and 34.5°, respectively, moreover, they vary in a relatively narrow range, that is, ∼15.6° (declination *S.D.*) and ∼10.3° (inclination *S.D.*). Both directional data show an interesting swing between 9060 and 9810 cal. yr BP where anomalous values in declination and inclination were found in all cores. Such result could be interpreted as a geomagnetic excursion or a very short reversal, however, further examination and other record would be necessary to confirm this interpretation.

A qualitative comparison between the SV curve and independent data from lava flow reveals a relative and reasonable agreement between them. Unfortunately, lava data are spread unevenly over the period under study, and so more independent data for comparison is needed.

On the other hand, there is a good agreement in shape and occurrence between the main inclination, and some declination features, found here with features in shown by SV master curves from Great Britain (UK), Fennoscandia (Sweden and Finland) and Great Lakes (USA). It is worth mentioning that the strong inclination swing found in this study coincides very well with features m and μ (lows in inclination) from the UK and Great Lakes master curves, which could support the existence of a short anomalous behaviour of the geomagnetic field around 9000–9800 cal. yr BP.

ACKNOWLEDGMENTS

The authors thank the Universidad Nacional Autonoma de Mexico (UNAM), the University of California Berkeley (UCLA), the GeoForschungsZentrum Potsdam (GFZ), the CONICET and Universidad Nacional del Centro de la Provincia de Buenos Aires (UNCPBA). The authors are greatly indebted to M Sc. A. Irurzun, Drs C. Gogorza and A. Sinito from the UNCPBA for their help and useful suggestions. They also thank to M Sc. D. Michalk from the GFZ for his help. The anonymous reviewers are thanked for their critical comments. Dr M. Chaparro was supported by a Postdoctoral Fellowship (DGPA-UNAM 2007–2008) from the UNAM. Financial support was also received from UNAM-PAPIIT project IN119399, UCMEXUS and the Stahl and Larsen Foundations at the UCLA.

REFERENCES

Aharon, P., 2003. Meltwater flooding events in the Gulf of Mexico revisited: implications for rapid climate changes during the last deglaciation, *Paleoceanography,* **18**(4), 1079, doi:10.1029/2002PA000840.

Alcocer, J., Escobar, E. & Lugo, A., 2000. Water use (and abuse) and its effects on the crater-lakes of Valle Santiago, Mexico, *Lakes & Reservoirs: Res. Manag.,* **5,** 145–149.

Barajas-Gea, C.I. & Rodriguez-Vargas, J.L., 2005. Fechamiento y estudio paleomagnético de rocas volcánicas en el campo volcánico Michoacán – Guanajuato, *Unpublished thesis,* Instituto Tecnológico Cd. Madero, Madero City (México), 63 pp.

Böhnel, H.N. & Molina-Garza, R.S., 2002. Secular variation in Mexico during the last 40,000 years, *Phys. Earth planet. Inter.,* **133,** 99–109.

Butler, R.F., 2004. Paleomagnetism: Magnetic domains to geologic terranes, Electronic edition, http://www.geo.arizona.edu/Paleomag/book/

Bradbury, J.P., 2000. Limnologic history of Lago de Patzcuaro, Michoacan, Mexico for the past 48,000 years: impacts of climate and man, *Palaeogeogr., Palaeoclimatol., Palaeoecol.,* **163,** 69–95.

Brown, R.B., 1984. The paleocology of the northern frontier of Mesoamerica, Unpublished PhD thesis, University of Arizona.

Creer, K.M., 1983. Computer synthesis of geomagnetic palaeosecular variations, *Nature,* **304,** 695–699.

Creer, K.M. & Tucholka, P., 1982a. Construction of type curves of geomagnetic secular variation for dating lake sediments from east central North America, *Can. J. Earth Sci.,* **19,** 1106–1115.

Creer, K.M. & Tucholka, P., 1982b. Secular variation as recorder in lake sediments: a discussion of North American and European results, *Philos. Trans. R. Soc. Lond. A,* **306,** 87–102.

Creer, K.M., Tucholka, P. & Barton, C.E., 1983a. Paleomagnetism of lake sediments, in *Geomagnetism of Baked Clays and Recent Sediments,* pp. 172–197, eds Creer, K.M., Tucholka, P., Barton, C.E., Elsevier, Amsterdam.

Creer, K.M., Valencio, D.A., Sinito, A.M., Tucholka, P. & Vilas, J.F., 1983b. Geomagnetic secular variations 0–14000 years BP as recorded by lake sediments from Argentina, *Geophys. J. R. Astron. Soc.,* **74**(1), 109–222.

Day, R., Fuller, M. & Schmidt, V.A., 1977. Hysteresis properties of titanomagnetites: grain size and compositional dependence, *Phys. Earth planet. Inter.,* **13,** 260–267.

Ferrari, L., Conticelli, S., Vaggelli, G., Petrone, C.M. & Manetti, P., 2000. Late Miocene volcanism and intra-arc tectonics during the early development of the Trans-Mexican Volcanic Belt, *Tectonophysics,* **318,** 161–185.

Fisher, R.A., 1953. Dispersion on a sphere, *Proc. R. Soc., Lond., Ser. A,* **217,** 295–305.

Gogorza, C.S., Sinito, A.M., Di Tomasso, I., Vilas, J.F., Creer, K.M. & Nuñez, H., 1999. Holocene secular variation recorded by sediments from Escondido Lake (south Argentina), *Earth Planets Space,* **51,** 93–106.

Gonzalez, S., Sherwood, G., Böhnel, H. & Schnepp, E., 1997. Paleosecular variation in central Mexico over the last 30,000 years: the record from lavas, *Geophys. J. Int.,* **130,** 201–219.

Hillesheim, M.B. *et al.*, 2005. Climate change in lowland Central America during the late deglacial and early Holocene, *J. quarter. Sci.,* **20**(4), 363–376.

Haug, G.H., Hughen, K.A., Sigman, D.M., Peterson, L.C. & Röhl, U., 2001. Southward migration of the Intertropical Convergence Zone through the Holocene, *Science,* **293,** 1304–1308.

Irurzun, M.A., Gogorza, C.S., Chaparro, M.A.E., Lirio, J.M., Nuñez, H., Vilas, J.F. & Sinito, A.M., 2006. Paleosecular variations recorded by Holocene-Pleistocene sediments from Lake El Trebol (Patagonia, Argentina), *Phys. Earth planet. Inter.,* **154,** 1–17.

Kirschvink, J.L., 1980. The least-squares line and plane and the analyses of paleomagnetic data, *Geophys. J. R. Astron. Soc.,* **62,** 699–718.

Kruiver, P.P., Dekkers, M.J. & Heslop, D. 2001. Quantification of magnetic coercivity components by the analysis of acquisition curves of isothermal remanent magnetisation, *Earth planet. Sci. Lett.,* **189,** 269–276.

Liddicoat, J.C., Lambert, P.W. & Valastro, S. Jr., 1979. Paleomagnetic record in late Pleistocene and Holocene dry lake deposits at Tlapacoya, Mexico, *Geophys. J. R. Astron. Soc.,* **59,** 367–377.

Lund, S.P. & Baneerje, S.K., 1985. Late Quaternary field secular variation from two Minnesota lakes, *J. geophys. Res.,* **90,** 803–825.

Lund, S.P., Liddicoat, J.C., Lajoie, K.R., Henyey, T.L. & Robinson, S.W., 1988. Paleomagnetic evidence for long-term (10E+4 year) memory and periodic behavior in the easrth's core dynamo process, *Geophys. Res. Lett.,* **15,** 1101–1104.

Maher, B.A., 1986. Characterisation of soils by mineral magnetic measurements, *Phys. Earth planet. Inter.,* **42,** 76−92.

Murphy, G.P., 1982. The chronology, pyroclastic stratigraphy, and petrology of the Valle de Santiago Maar Field, Central Mexico, *MS thesis*, University of California, Berkeley.

Nowaczyk, N.R., 2001. Logging of magnetic susceptibility, in *Tracking Environmental Change Using Lake Sediments: Basin Analysis, Coring, and Chronological Techniques,* pp. 155–170, eds Last, W.M. & Smol, J.P., Kluwer Academic publishers, Dordrecht.

Ojala, A.E.K. & Tiljander, M., 2003. Testing the fidelity of sediment chronology: comparison of varve and paleomagnetic results from Holocene lake sediments from central Finland, *Quarter. Sci. Rev.,* **22,** 1787–1803.

Ortega-Guerrero, B., 1992. Palaeomagnetismo, magnetoestratigrafia y paleoecologia del Cuaternario tardio en el Lago de Chalco, Cuenca de Mexico, *PhD thesis*. UNAM, Mexico City, 161 pp.

Ortega-Guerrero, B. & Urrutia-Fucugauchi, J., 1997. A palaeomagnetic secular variation record from late Pleistocene-Holocene lacustrine sediments from Chalco Lake, Basin of Mexico, *Quater. Int.,* **43–44,** 87–96.

Park, J., 2005. Hololcene climate change and human environmental impacts in Guanajuato, Mexico, *PhD thesis*, University of California, Berkely, 150 pp.

Peng, L. & King, J.W., 1992. A late Quaternary geomagnetic secular variation record from Lake Waiau, Hawaii, and the question of the Pacific nondipole low, *J. geophys. Res.,* **97**(B4), 4407–4424.

Peters, C. & Dekkers, M., 2003. Selected room temperature magnetic parameters as a function of mineralogy, concentration and grain size, *Phys. Chem. Earth,* **28,** 659–667.

Snowball, I., Zillén, L., Ojala, A., Saarinen, T. & Sandgren, P., 2007. FENNOSTACK and FENNORPIS: Varve dated Holocene paleomagnetic secular variation and relative palaeointensity stacks from Fennoscandia, *Earth planet. Sci. Lett.,* **255,** 106–116.

Stockhausen, H., 1998. Some new aspects for the modelling of isothermal remanent magnetization acquisition curves by cumulative log Gaussian functions, *Geophys. Res. Lett.,* **25**(12), 2217–2220.

Stuiver, M. *et al.*, 1998. INTCAL98 radiocarbon age calibration, 24,000–0 cal BP, *Radiocarbon,* **40,** 1041–1083.

Stuiver, M., Reimer, P.J. & Reimer, R.W., 2005. CALIB 5.0 [www program and documentation].

Turner, G.M. & Thompson, R., 1979. Behaviour of the Earth's magnetic field as recorded in the sediment of Loch Lomond, *Earth planet. Sci. Lett.,* **42,** 412–426.

Turner, G.M. & Thompson, R., 1981. Lake sediment record of the geomagnetic secular variation in Britain during Holocene time. *Geophys. J. R. Astron. Soc.,* **54,** 703–725.

Turner, G.M. & Thompson, R., 1982. Detransformation of the British geomagnetic secular variation record for Holocene times, *Geophys. J. R. Astron. Soc.,* **70,** 789–792.

Verosub, K.L., Mehringer, P.J. & Waterstraat, P., 1986. Holocene secular variation in western North America: paleomagnetic record from Fish Lake, Harney County, Oregon, *J. geophys. Res.,* **91,** 3609–3623.

Vigliotti, L., 2006. Secular variation record of the Earth's magnetic field in Italy during the Holocene: constraints for the construction of a master curve, *Geophys. J. Int.,* **165,** 414–429.

Vlag, P., Alva-Valdivia, L., de Boer, C.B., Gonzalez, S. & Urrutia-Fucugauchi, J., 2000. A rock- and paleomagnetic study of a Holocene lava flow in central Mexico, *Phys. Earth planet. Inter.,* **118**(3–4), 259–272.

Zijderveld, J.D.A., 1967. AC demagnetization of rocks: analysis of results, in *Methods in Palaeomagnetism,* pp. 254–286, eds Collinson, D.W., Creer, K.M. & Runcorn, S.K., Elsevier, New York, NY.